4 SEEPS AND DAMP SPOTS

4.1 South Ramp Seepage Observations

Yucca Mountain Project staff collected a set of water samples between March 2, 2005, and May 5, 2005, from water seeping from faults and fractures in the South Ramp of the Exploratory Studies Facility (ESF)[1] (Bechtel SAIC Company, LLC, 2005). This seepage occurred at locations underlying surface exposures of units that exhibit little infiltration in the Infiltration Tabulator for Yucca Mountain (ITYM)[2] model because of relatively low fracture intensities. Bechtel SAIC Company, LLC (2005) reports that the collection period followed a 5-month period from October 2004 through February 2005, with cumulative precipitation of 324 mm [12.75 in] at Yucca Mountain Project meteorological monitoring Site 1; this was approximately 3.5 times the average for the same months over the prior decade (Bechtel SAIC Company, LLC, 2005). The seepage was noticed on February 28, 2005, during a biweekly inspection but was not noticed on February 24, 2005—the previous time personnel passed the seep locations. Figure 4-1 summarizes the sequence of events, including precipitation and calculated Penman evapotranspiration at the Site 1 meteorological station (NTS 60) located approximately 1.8 km [1.1 mi] north-northwest of the seep locations. The Site 8 meteorological station (Knothead Gap) is approximately 1.2 km [0.75 mi] east of the South Portal; a rainy-day precipitation measurement is missing at Site 8 during the sequence of rainy days prior to the first observation of seepage, but the precipitation sequences are quite similar and cumulative precipitation agrees to within 2 percent.

According to Bechtel SAIC Company, LLC (2005), early in the event the fracture system between stations 75+60 and 76+05 was generally wet at the drift's crown and flowed down the ribs in several places. Seeps between stations 75+62 and 76+04 emanated from faults and fracture sets, and the seep at station 77+52 entered at the crown and flowed down the left rib following a fault. Figure 4-2 reproduces the seepage locations within the ESF mapped on February 28, 2005, and Figure 4-3 illustrates the position of the seep locations relative to damp features and surface exposures of rock units as Day, et al. (1998) mapped. Figure 4-3 also illustrates the position of the same geochemical observations illustrated in Figures 3-1 through 3-3, with the observations drawn offset from the drift for better visibility. The maximum initial flow rate was reported to be 125 ml/hr [0.033 gal/hr], dropping to 6.7 ml/hr [0.0018 gal/hr] in late April and early May. Active seepage was limited to stations 75+75, 75+94, and 75+95 by late April and ceased during the second week of May. The seeps with largest reported sample volumes were between stations 75+89 and 76+01, with >500 ml [0.13 gal] samples collected in at least 6 locations and >200 ml [0.053 gal] samples collected in at least 13 locations (Bechtel SAIC Company, LLC, 2005, Table A1). The largest reported seep sample between stations 75+62 and 75+82 was much smaller, 40 ml [0.01 gal] at station 75+75, although Bechtel SAIC Company, LLC (2005, Table A1) does not report sample volume for most samples in this part of the ESF. Bechtel SAIC Company, LLC (2005, Table A1) does not report sample volumes for the two samples collected from the seep at station 77+52; the last collection from this seep was on March 15, 2005. The samples with geochemical analyses Oliver and Whelan (2006) and Cizdziel, et al. (2008) reported were collected between stations 75+73 and 76+00.5 and at station 77+52, with locations indicated in Figure 4-1.

[1]Exploratory Studies Facility is used frequently throughout this report; therefore, the acronym ESF will be used.
[2]Infiltration Tabulator for Yucca Mountain is used frequently throughout this report; therefore, the acronym ITYM will be used.

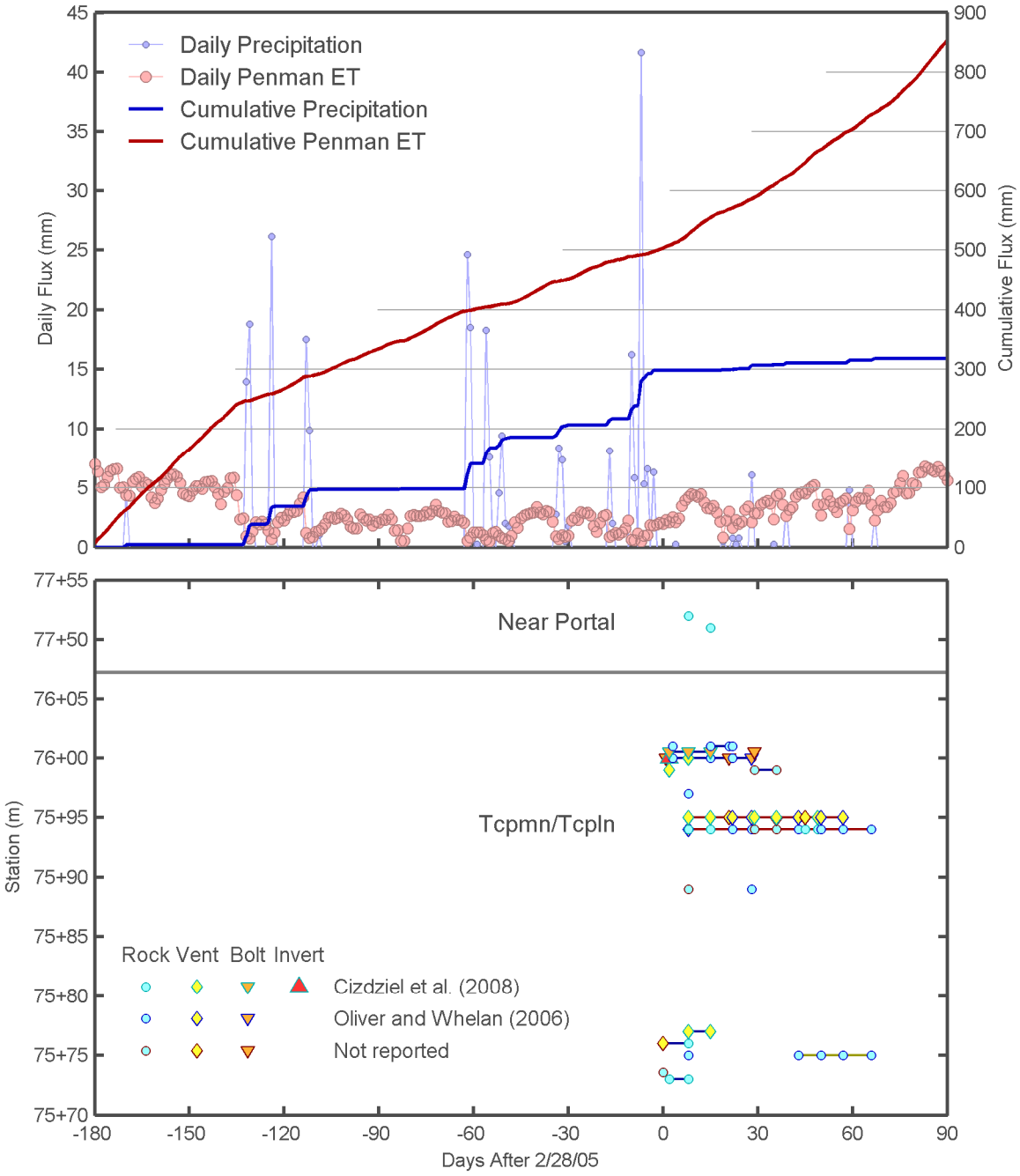

Figure 4-1. Time History of Daily and Cumulative Site 1 Precipitation and Penman Evapotranspiration and Seepage Measurements

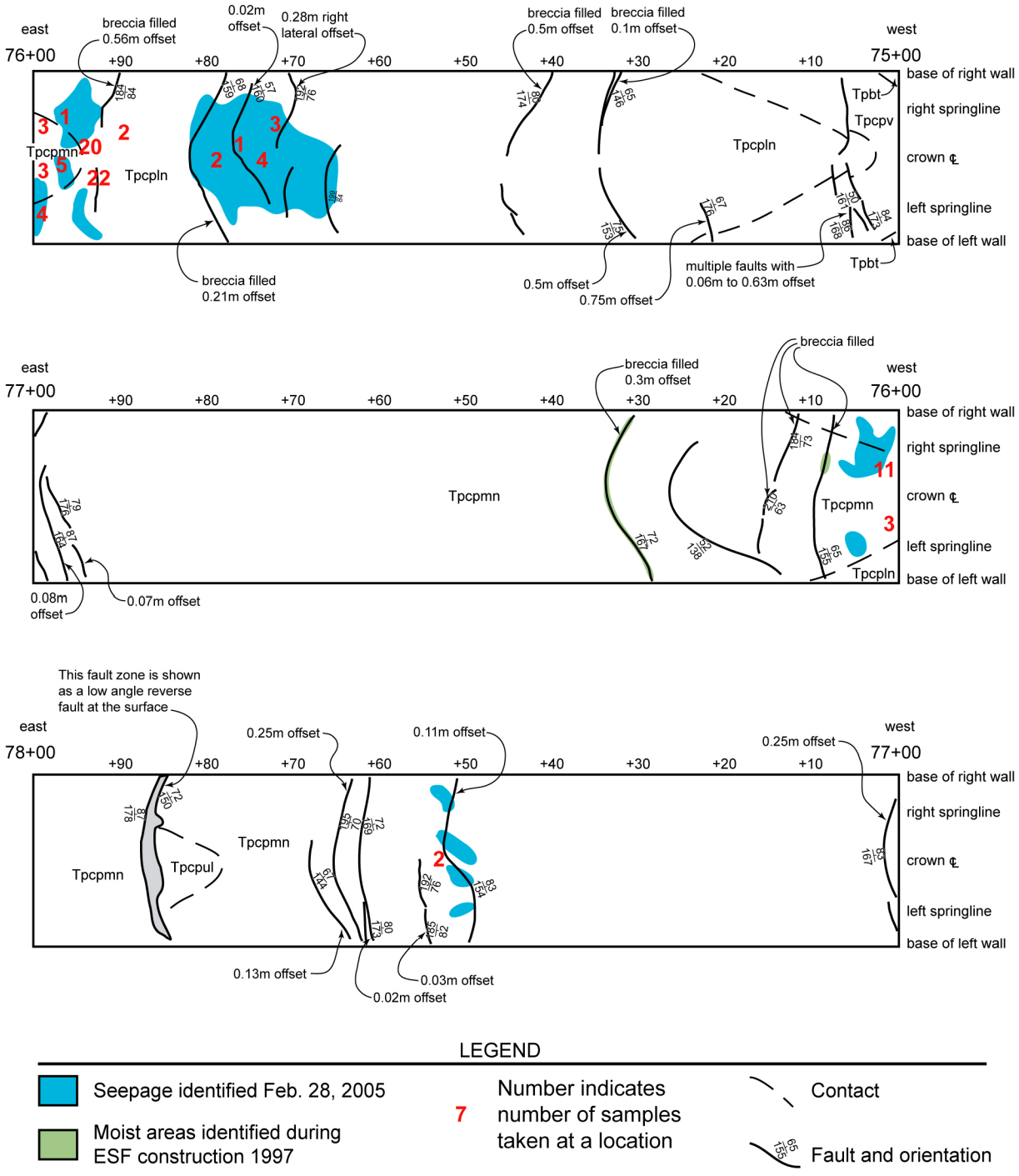

Figure 4-2. Full-Periphery Map Displaying Locations of Seeps and Damp Spots (Reproduced From Bechtel SAIC Company, LLC, 2005, Figure 1)

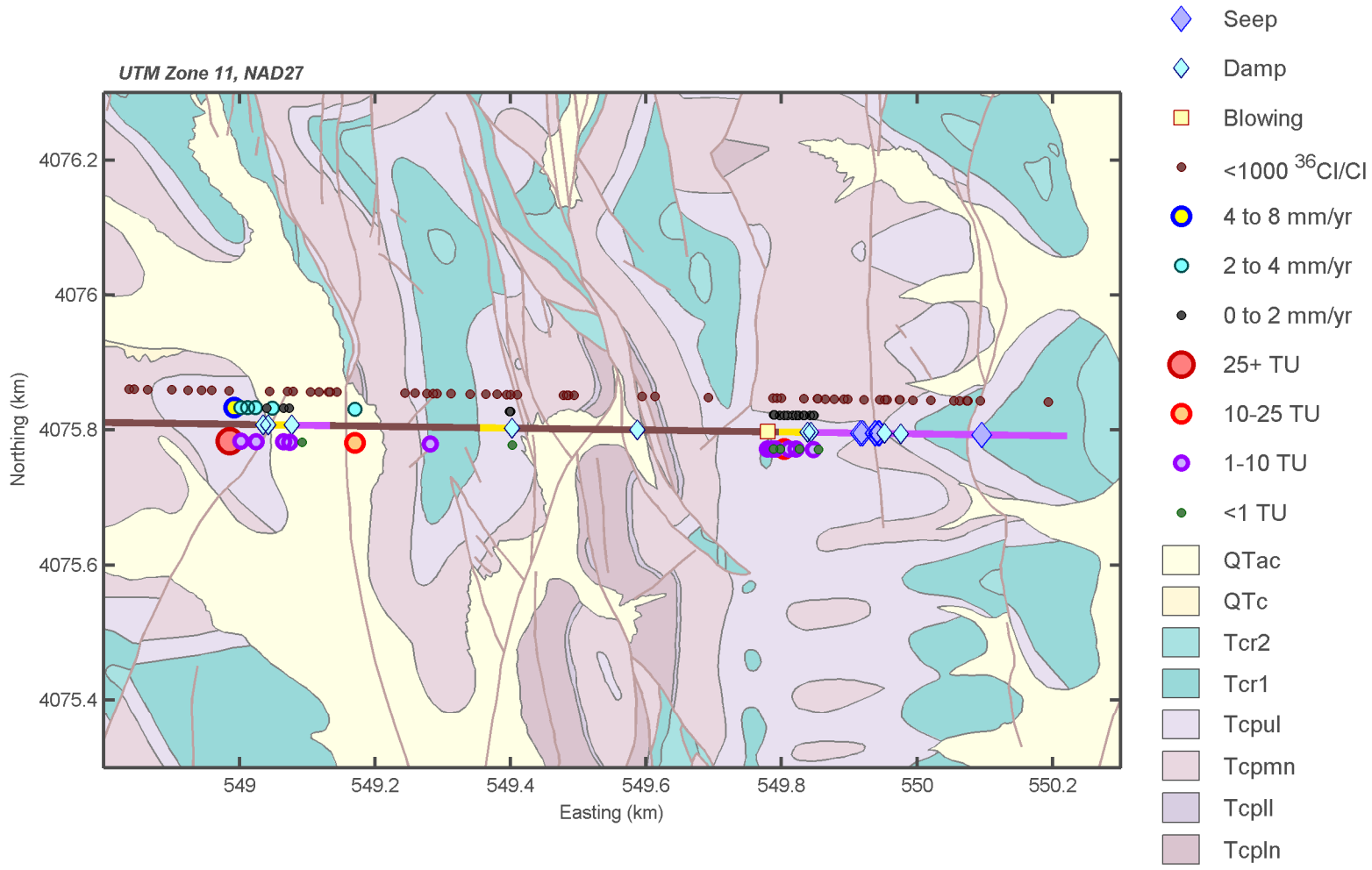

Figure 4-3. Features in the South Ramp of the Exploratory Studies Facility. Seep Samples, Damp Features, and the Blowing Fracture Are Drawn Over the Drift. Chlorine-36, Tritium, and Chloride Observations Drawn From Figures 3-1 Through 3-3 of This Report Are Offset For Visibility. [1 km = 0.62 mi; 25.4 mm/yr = 1 in/yr; 1 mg/L = 1 ppm]

The average concentration Oliver and Whelan (2006, Table II) and Cizdziel, et al. (2008, Table 3) reported at each seep location is shown plotted by station in Figure 4-4. Components with most or all values below detection limits are not plotted. Each concentration value is normalized by the average value of the species near station 77+52 to facilitate comparisons. Some of the components, particularly manganese, appear sensitive to whether the water sample was obtained before or after it contacted manufactured materials such as a rock bolt, vent, or the concrete invert. The spike in Ca, K, Mg, and Na at station 76+00 is from two early samples from the drift crown at station 76+00, collected on March 3 and 8, 2005, that Cizdziel, et al. (2008, Table 3) documented.

Trends in the chemistry between stations 75+73 and 76+00.5 do not appear to project to the samples near station 77+52 for many of the species. Depth below the ground surface represents a measure of travel distance for vertical flow. The depth of each sample was estimated by digitizing the South Ramp as-built cross section Bechtel SAIC Company, LLC (2005, Plate 1) presented. The slope of the ground surface changes between stations 76+00.5 and 77+52, although the depth decreases monotonically for these stations. The samples may better fall within the trends when plotting the samples by depth (Figure 4-5), but based on Figures 4-4 and 4-5, these samples may have a different source of infiltrating water.

Chloride is often used to estimate infiltration fluxes because it is considered to reflect relatively minimal interactions with the rock mass (i.e., with the matrix or fill materials), and Yucca Mountain tuffs are not thought to be a significant source of chloride because the tuffs are low in chloride (CRWMS M&O, 2003). Sulfate (SO_4) is another species that may have minimal interactions with the rock. With similar precipitation source concentrations and without rock–mass interactions, the increase in chloride concentrations with distance from the South Portal shown in Figure 4-4 implies increased evaporation, consistent with interpretations of stable isotope observations in the seep waters Oliver and Whelan (2006) presented. Because the ratio of other chemical species to chloride is unaffected when a water sample evaporates (unless the species becomes so concentrated that it begins to precipitate), differences in the ratio of a species to chloride between two seep samples implies that the samples interacted with the soil and rock to different extents.

Figure 4-6 presents a representative subset of data shown in Figure 4-4 in the form of the average ratio of the component concentration to the chloride concentration of the sample. The ratios are presented according to depth as a measure of vertical travel distance. The ratios of K, Na, and Mg to chloride each approximately halve over 8 m [26 ft], but the ratios of Ca and SO_4 to chloride change by a much smaller amount. Geochemical trends from boreholes would provide a point of comparison, but there are few borehole geochemical pore-water samples available from the Tiva Canyon welded (TCw)[3] and Topopah Spring welded (TSw)[4] units. Borehole SD-9 has a relatively large number of geochemical samples through the TSw unit. In borehole SD-9 (see Figure 3-4), Na and K are more concentrated and Ca, Mg, and SO_4 are less concentrated relative to chloride at the base of the TSw unit than at the base of the Paintbrush Tuff nonwelded (PTn)[5] unit, a distance of approximately 325 m [1,070 ft]. The Ca, Na, and K ratios at the base of the TSw are within a factor of two relative to the ratios at the base of the PTn, SO_4 is more dilute by approximately a factor of four, and Mg is more dilute by

[3]Tiva Canyon welded is used frequently throughout this report; therefore, the acronym TCw will be used.
[4]Topopah Spring welded is used frequently throughout this report; therefore, the acronym TSw will be used.
[5]Paintbrush Tuff nonwelded is used frequently throughout this report; therefore, the acronym PTn will be used.

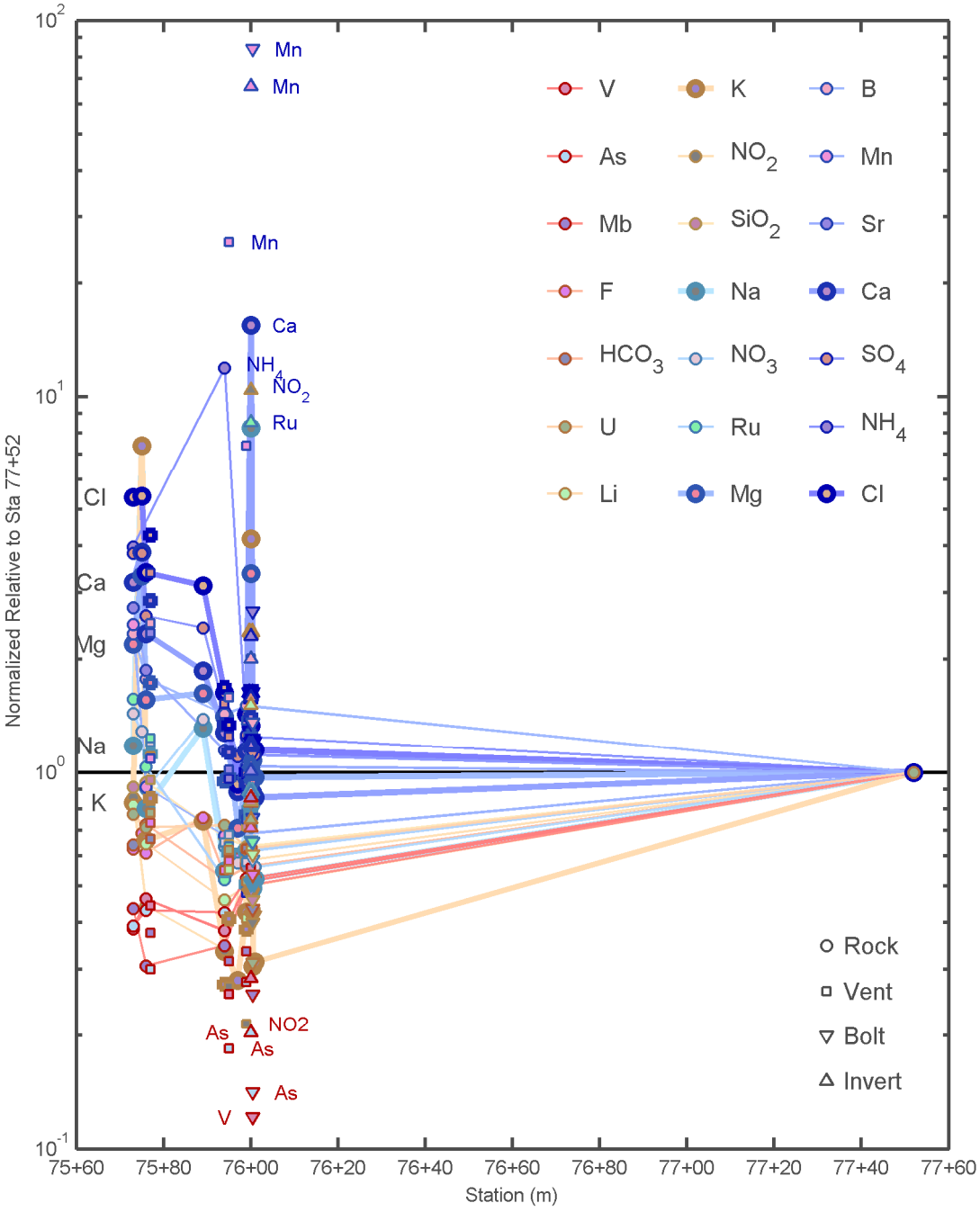

Figure 4-4. Mean Observed Concentration at Each Seep Location, Plotted by Station [1 ft = 0.3048 m]

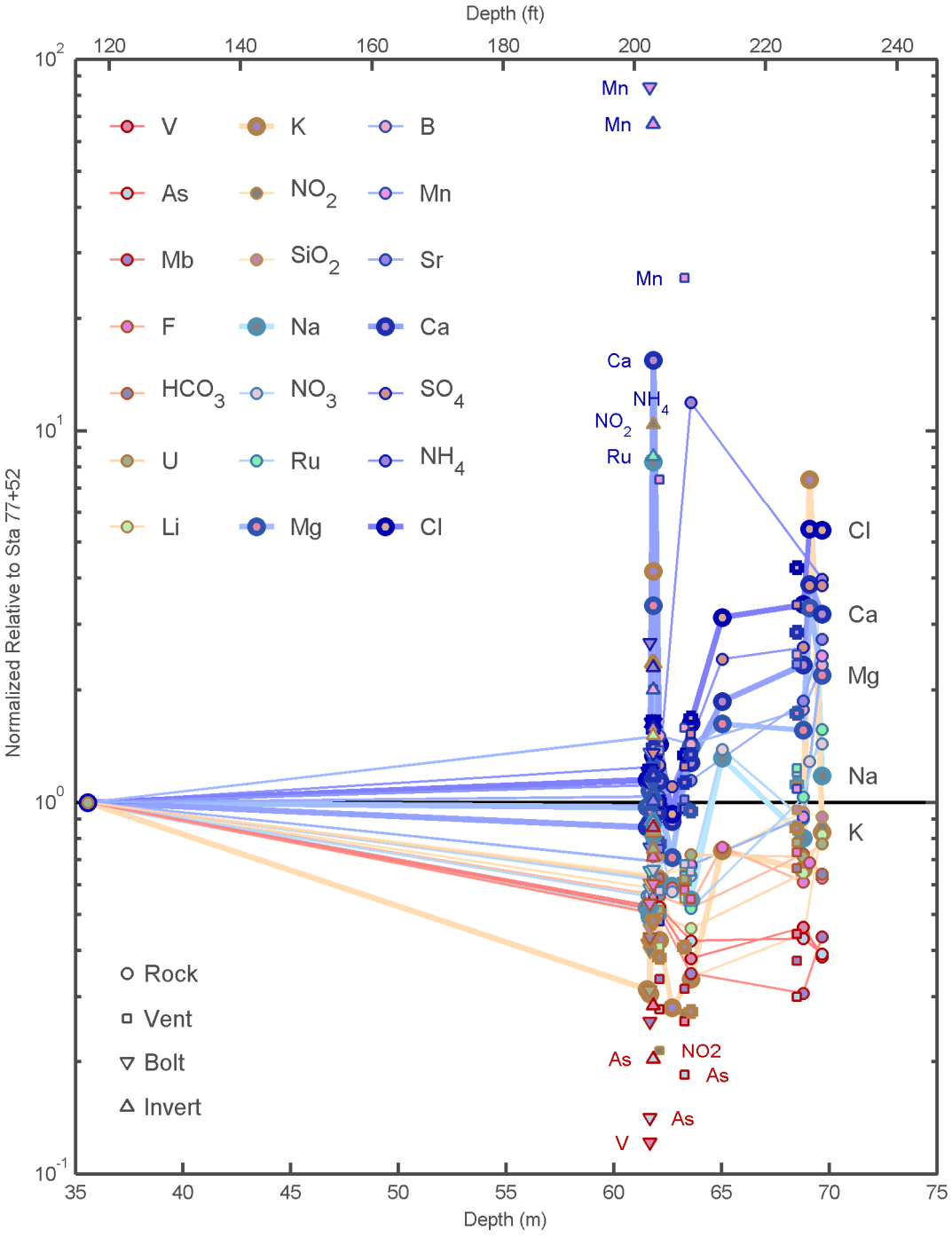

Figure 4-5. Mean Observed Concentration at Each Seep Location, Plotted by Depth Below Ground Surface

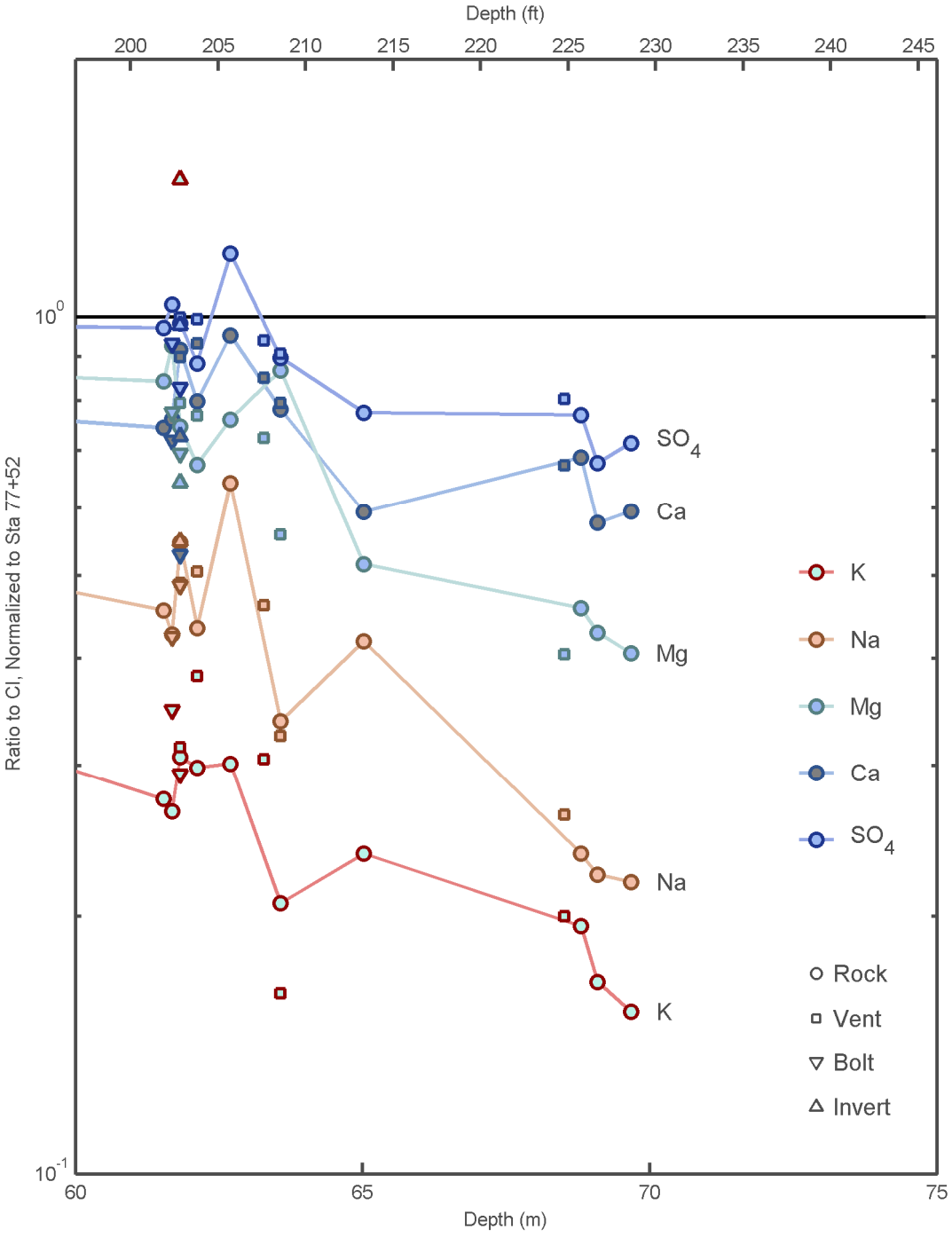

Figure 4-6. Mean Observed Concentration of Selected Species at Each Seep Location Between Stations 75+62 and 76+00.5

approximately an order of magnitude. In summary, the rate of change in chemistry with depth is much larger at the seeps than in the SD-9 TSw; Ca, Mg, and SO_4 become more dilute with respect to chloride as depth increases in both locations; and Na and K change in opposite directions with respect to chloride at the two locations.

Water samples collected from the South Ramp seeps had chloride concentrations between 41.3 and 236 mg/L [41.3 and 236 ppm] (Bechtel SAIC Company, LLC, 2005, Table A2; Oliver and Whelan, 2006, Table II; Cizdziel, et al., 2008, Table 3). The seepage-water chloride concentrations correspond to q_w values between 1.6 and 0.27 mm/yr [0.063 and 0.011 in/yr], respectively, using the representative present-day values. CRWMS M&O (2003) estimates the effective chloride concentration for rainfall at Yucca Mountain (including both wet and dry deposition) to be approximately 0.35 mg/L [0.35 ppm]. The two to three orders of magnitude increase in sample chloride concentration relative to the effective rainfall chloride concentration implies that the samples must contain chloride deposited prior to the rainfall events unless more than 99 percent of the water entering the ground was lost due to evaporation during the cool winter and spring months of the event. However, Figure 4-1 suggests that during the last 2 months prior to the seepage event, potential evapotranspiration (which is an upper bound for actual evapotranspiration) is only sufficient to remove half of the rainfall in the period, and this rainfall represents approximately two-thirds of the rainfall during the 6 months prior to the event.

The remainder of Section 4 presents hypotheses for why the seeps occurred where they did and what infiltration characteristics are implied by the seep characteristics. Sections 4.2 through 4.4 describe additional related observations and site characteristics. Sections 4.5 through 4.7 present three hypotheses for the seep characteristics that are tied to site and infiltration characteristics unique to the seep zone, and Section 4.8 summarizes and contrasts the hypotheses.

4.2 Exploratory Studies Facility Damp Spots and Blowing Fracture

Eatman, et al. (1997) noted dampness at nine locations in the TCw, PTn, and TSw units, observed prior to geologic mapping during the excavation of the South Ramp, including dampness at stations 76+08 (in a fracture) and 76+32 (in a fault with “a rather large breccia zone across much of the tunnel”). The damp features are indicated in Figure 4-3. The damp features may be associated with the same conditions leading to the seepage events, especially the first location because of its proximity. Five of the damp features (at stations 66+91, 66+95 to 67+01, 67+32, 70+58, and 72+43) are within 20 m [66 ft] of a fault mapped at the ground surface at the base of a hill slope, another is within 20 m [66 ft] of an inferred fault that is mapped intersecting a channel approximately 30 m [98 ft] perpendicular to the dip direction (at 76+08), and another (at 76+32) is mapped approximately 35 m [115 ft] downdip of the same fault. All faults with shallow soil and an upslope contributing area have damp or seeping features within approximately 20 m [66 ft]; no faults mapped in alluvium have a wet feature associated with them. Note that Day, et al. (1998) map more extensive faulting in the South Ramp area than in the potential repository footprint.

Damp features were found at each South Ramp location where the base of the TCw meets the PTn and at one of the two North Ramp locations. Two of the damp South Ramp contact features (at stations 66+95 to 67+01 and 67+32) are associated with a mapped surficial fault; the two damp features at stations 74+95 and 75+00 are the only two of the nine not associated with any mapped surficial fault. The South Ramp contact features were damp within the matrix,

as was the North Ramp feature. Soeder (1995) described the North Ramp damp feature a short distance past station 7+63: "[a] number of fractures visible near the ring erector in the crown and along both ribs above spring line were stained dark, as though damp. The rock below spring line is virtually unfractured, and appeared uniformly damp in the matrix."

The North Ramp feature is located under the boundary between the Tcr1 and Tcr2 zones, approximately 60 m [200 ft] downdip of a small fault-induced channel and 40 m [130 ft] updip of a fault inferred by Day, et al. (1998). Little lateral water movement is needed under the hypothesis that the water for the North Ramp feature infiltrated within the Tcr2 unit; the hypothesis that the water originated from a mapped fault implies lateral movement of 40 to 60 m [130 to 200 ft] above the PTn. The South Ramp damp features at stations 74+95 and 75+00 underlie an outcrop of lithophysal Tcpul without any mapped fault, and are approximately 40 and 65 m [130 and 210 ft] from the highest reaches of ephemeral channels that Day, et al. (1998) mapped as incised into the Tcpul and Tcpmn zones, respectively.

Eatman, et al. (1997) described an "exhaling" fracture at station 74+36, with the blowing air noticeably cooler than the tunnel air. As shown in Figure 4-3, the fracture is at the top of the TSw just under the PTn/TSw transition. Eatman, et al. (1997) infer that the blowing fracture implies a somewhat direct connection to the surface through the overlying units; the nearest Day, et al. (1998)-mapped surface fault lies approximately 40 m [130 ft] northwest of the blowing fracture location. The 74+95 and 75+00 damp spots at the TCw/PTn transition would require 90 m [300 ft] of downdip travel if they were directly connected to the fault nearest the blowing fracture. The chlorine-36 and chloride observations between the blowing fracture and the damp spots are uniformly indicative of low water movement through the PTn, but most of the tritium observations between the blowing fracture and the damp spots have concentrations >1 TU, with a maximum value of 12.5 TU. The tritium samples may have been obtained from different liquid pathways than the chlorine-36 and chloride samples, or tritium may have spread from liquid pathways within the vapor phase. The elevated tritium concentrations, which are generally below present-day atmospheric concentrations, may also be associated with atmospheric air (and its relatively large tritium concentrations) penetrating the PTn through the system feeding the blowing fracture.

Unlike the ESF, the entire length of the Enhanced Characterization of the Repository Block (ECRB)[6] is within the TSw unit, and is overlain by the TCw and PTn units over all but the westernmost reach. No direct observation of a seepage event or wet fracture has been reported in the ECRB. Geochemical sample locations in the ECRB are overlain by a mix of lithophysal, nonlithophysal, and caprock units, in order of increasing potential for infiltration in the ITYM model (Stothoff, 2008a). Every ECRB sample has at least two different types of units cropping out within a 50-m [164-ft] horizontal radius of the sample, except for 5 samples clustered under the Tcr2 zone on Yucca Crest. The geochemical samples are characterized by local variability and exhibit only limited indications of higher flux pathways.

4.3 South Ramp Lithology and Topology

The full-periphery figure describing the seep locations (Figure 4-2) suggests that the seeps can be grouped into a primary seepage zone (stations 75+62 through 76+04) and a secondary

[6]Enhanced Characterization of the Repository Block is used frequently throughout this report; therefore, the acronym ECRB will be used.

seepage zone (stations 77+48 through 77+52). A single contiguous wet area is drawn between stations 75+62 and 75+82 in the primary seepage zone, with several smaller wet areas indicated between stations 75+89 and 76+04. The full-periphery figure indicates that the wet zones approximately between stations 75+95 and 75+62 occur in the Tcpln unit and the seeps between station 75+95 and the South Portal occur within the Tcpmn unit. Two of the longest lived seeps occurred at the contact between the Tcpmn and Tcpln units. The full-periphery figure indicates that seep locations are more or less equally distributed on the left and right walls of the drift. A geologic cross section for the as-built South Ramp (Bechtel SAIC Company, LLC, 2005, Plate 1) indicates that the Tcpll unit, which normally lies between the Tcpmn and Tcpln units, crops out on the west face of Boundary Ridge but pinches out updip of the drift. This cross section also indicates that the fault near the secondary seep location passes above the seep locations.

Stothoff (2008a) suggests that nonlithophysal units (e.g., the Tcpmn and Tcpln units) are more favorable for infiltration than lithophysal units (e.g., the Tcpul and Tcpll units) because nonlithophysal units tend to exhibit greater fracture intensities. Day, et al. (1998) maps three lithological units as exposed above the ESF between the crest of Boundary Ridge, approximately at ESF station 73+50, to the South Portal at ESF station 78+77. At the ground surface along the path of the ESF, the Tcpul unit is mapped from the crest of Boundary Ridge to approximately station 75+75, stations 76+08 to 76+58, and stations 77+32 to 77+45; the Tcpmn unit is mapped from stations 75+75 to 76+08; and the Tcr1 unit is mapped from stations 76+58 to 77+32 and 77+45 to the South Portal. The Tcpmn unit is also exposed at the surface for approximately 50 m [160 ft] on the west side of the Boundary Ridge crest.

The primary seepage zone, between stations 75+62 and 76+04, appears to be closely associated with the mapped exposure of the Tcpmn unit (approximately from stations 75+75 to 76+08). Part of the primary seepage zone lies directly under the mapped exposure. The portion of the zone between stations 75+62 and 75+75 (west, or updip, of the mapped Tcpmn exposure) may also be associated with the mapped exposure, because faults in this zone project into the exposure. The 3 mapped features with nonzero offset between 75+62 and 75+85 dip between 68° and 77° to the west, according to the detailed line survey Eatman, et al. (1997) reported. Overburden thicknesses to the ESF spring line, as digitized from Bechtel SAIC Company, LLC (2005, Plate A1), are approximately 72.9 and 67.1 m [239 and 220 ft] at stations 75+62 and 75+82, respectively. Faults with angles between 68° and 77°, if extended from the ESF crown to the ridgeline, would intersect the ground surface within the mapped Tcpmn exposure between ESF stations 75+78.2 and 76+08.

The primary seepage zone is approximately 27 m [100 ft] north of a small channel cut into the Tcpmn near the base of a Tcpul exposure, with the channel incised 4 to 6 m [13 to 20 ft] relative to the ridgeline (Stothoff, 2008b). If water from this southern channel contacted the crown of the ESF at station 76+00, it would have traveled 27 m [100 ft] laterally and at least 53 m [164 ft] vertically—a spreading angle of 27° from the channel. The nearest channel to the north is approximately 70 m [230 ft] from the ridgeline and incised 12 to 15 m [39 to 49 ft] from the ridgeline (Stothoff, 2008b), implying a spreading angle of approximately 60° from the channel. Day, et al. (1998) maps an inferred near-vertical fault cutting the ridge from channel to channel at approximately ESF station 75+93.

The secondary seep, at station 77+52, emanated from a fault that Day, et al. (1998) does not map at the surface. Day, et al. (1998) does map a steeply dipping surface fault juxtaposing

Tcpul and Tcr1 exposures approximately 20 m [66 ft] west of the seep location; the surface-mapped fault intersects the ESF approximately 35 m [115 ft] east of the seep location (Bechtel SAIC Company, LLC, 2005, Figure 1). Day, et al. (1998) maps the surface fault as forming a slight drainage channel down each side of the ridge starting from a topographic saddle at the ridgetop.

These observations suggest three hypothetical paths for the seep water in the primary seepage zone (i.e., between stations 75+60 and 76+04). These hypothetical pathways are illustrated in Figure 4-7. The predominantly vertical local distributed infiltration pathway is inspired by the observation that the seeps are essentially coincident with the mapped Tcpmn unit exposures at the surface, with the Tcpmn unit uninterrupted from surface to or almost to the drift. The channel infiltration pathway is inspired by the observation that two intermittent channels exist in the area, with both at a higher elevation than the seep locations and with the nearer channel offset horizontally by approximately 30 m [100 ft] from the seep locations. The downdip diversion pathway is inspired by the observation that the seeps occur in the vicinity of a contact between the overlying Tcpmn and underlying Tcpln unit, with the Tcpll unit pinching out some unknown distance updip. None of these lithologic configurations occurs in any other stretch of the ESF.

4.4 Alcove 1 Infiltration Test

The Alcove 1 infiltration test near the North Portal, described by Liu, et al. (2003), used controlled surface application rates to induce seepage into a subsurface opening approximately 30 m [100 ft] below the ground surface. Observations from the test may be compared to natural seepage events. Liu, et al. (2003) reports that water was applied to the surface in two test phases at variable rates between 0 and 5 cm/d [0 and 2 in/d], averaging approximately 2 cm/d [0.8 in/d], and indicates that the applied rates are less than the saturated hydraulic conductivity of the fracture system. The two test phases were separated by more than 6 months.

The Alcove 1 infiltration test, relative to the South Ramp seepage event, had (i) greatly prolonged infiltration events (application durations of 5 and 17 months instead of hours to days), (ii) approximately half the distance from surface to cavity, and (iii) less-fractured units from higher in the profile. Like the South Ramp event, the Alcove 1 test featured intervals with no water applied separating intervals with water applied. Overland flow was precluded from the Alcove 1 event by testing protocols, but may have occurred at the South Ramp event.

The Tcrn1 and Tcpul units, which overlie Alcove 1, tend to be less densely fractured than the Tcpmn unit. Core samples from the Tcpul and Tcrn1 units have average estimated matrix permeability 10 and 650 times larger, respectively, than core samples from the Tcpmn unit according to Flint (1998) (although the estimated permeabilities are small in both units relative to peak percolation fluxes from both events). The matrix pore space available for water storage per unit volume is 2 and 4.6 times larger for the Tcpul and Tcrn1 units, respectively, than for the Tcpmn unit, based on average core sample saturation and porosity from the Flint (1998) database. These properties suggest that, under initial conditions representative of ambient conditions, a given water volume introduced into identical fractures within the Tcpmn and Tcpul units will lose at least twice as much water to the Tcpul unit than the Tcpmn unit, because the Tcpul matrix has twice the excess storage capacity of the Tcpmn and transfer rates may be

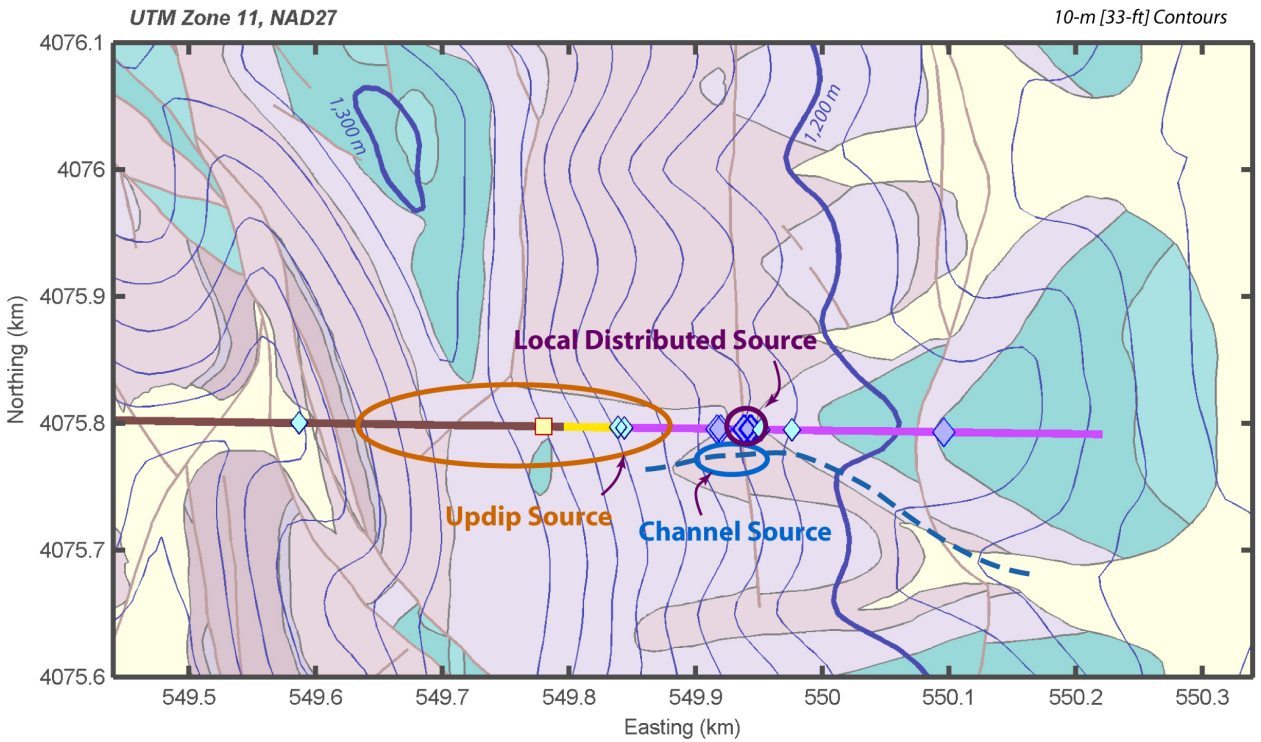

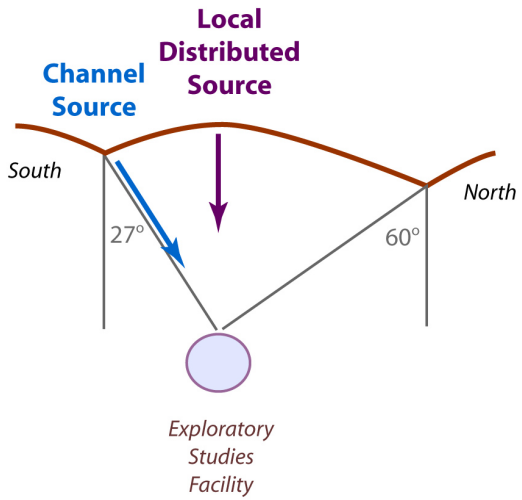

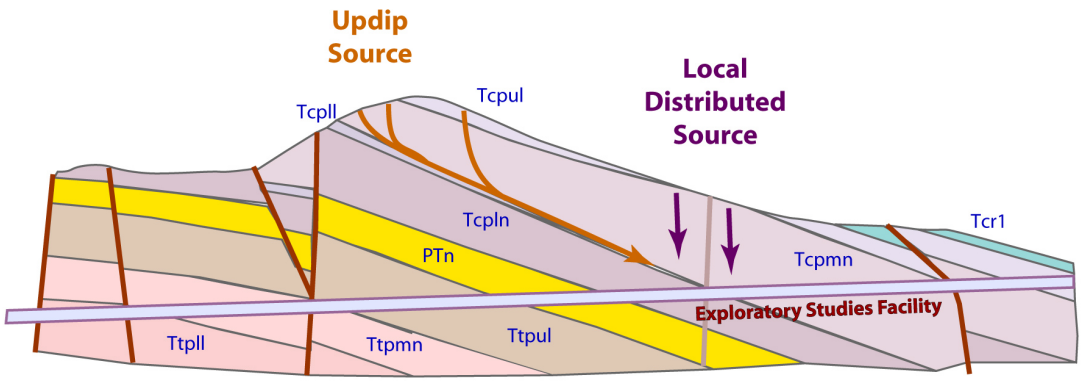

Profile redrawn from the South Ramp as-built geologic cross section (Bechtel SAIC Company LLC, 2005, Plate 1)

Bechtel SAIC Company LLC. "White Paper: South Ramp Water Seepage During February-May 2005." Las Vegas, Nevada: Bechtel SAIC Company, LLC. 2005.

Figure 4-7. Three Hypothesized Source Locations for the South Ramp Seepage Event

higher into the higher-permeability Tcpul. If conditions at the Alcove 1 and South Ramp sites are comparable to the core-sample database, wetting pulses at the South Ramp would be slowed less by matrix imbibition than wetting pulses at Alcove 1.

Seepage into Alcove 1, emplaced in the Tcpul unit approximately 30 m [100 ft] below the ground surface, started 75 days after initial surface application during the first phase and approximately 16 days after initial application in the second phase. Seepage ceased approximately 13 days after application stopped in the first phase. Liu, et al. (2003) do not report observations from the end of the second phase, but application ceased for a few weeks in two intervals within the second phase and the response trends suggest that seepage would have ceased approximately 2 to 3 weeks after the application stopped. Seepage rates typically responded to increases in application rate within a few days to 2 weeks, responding more quickly at larger application rates. These observations imply that, once the system is wet, seepage events are delayed by 2 to 3 weeks from an infiltration pulse and seepage duration is similar to the application period.

A bromide tracer was applied to the water in two pulses during the second phase. The first tracer pulse started 182 days after the start of the second infiltration phase and lasted 41 days; first breakthrough occurred approximately 40 days after the start of the pulse. After a hiatus of 113 days, the second pulse lasted 86 days. Breakthrough of the second pulse occurred 30 to 50 days after the start of the second pulse (Liu, et al., 2003, Figure 5), with breakthrough uncertainty arising from the possible observation of tracer from the first pulse. The centroid of the second pulse is observed in seep waters approximately 70 to 90 days after application (Liu, et al., 2003, Figure 5), suggesting that pressure responds 4 to 5 times faster than solute concentrations in this system. The comparison between pressure responses and solute responses suggests that two distinct response times can be applied to this system: (i) the hydraulic (or pressure) response time and (ii) the water travel time.

The Alcove 1 infiltration test shows an initial hydraulic response at the alcove that is almost five times faster in the second phase, once the system has been wetted with the first infiltration phase, suggesting that substantial transfer of water into storage delayed the first seepage response. Once the system was wetted with the first infiltration phase, the hydraulic response was approximately two to three times faster than the initial tracer response, suggesting that the initial water seeping into Alcove 1 was water in the system from the first phase that was displaced during the second phase. Once wetted, the hydraulic response time was 2 to 3 weeks, compared to 10 to 13 weeks for the mean tracer response time, so that seepage responded approximately 4 to 5 times faster than the dissolved solutes in the water.

The Alcove 1 infiltration test suggests that the fractured system responds relatively quickly to changes in infiltration once the limited amount of storage in the system is filled. The end of seepage at any particular location appears to be related to the end of the infiltration event, delayed by the hydraulic response time. The initiation of seepage at any particular location appears to be related to antecedent conditions; under dry antecedent conditions, seepage may take several times longer than the hydraulic response time, but under wet antecedent conditions seepage may initiate even faster than it stops after the end of infiltration. At Alcove 1, the seepage duration is comparable to the infiltration duration, perhaps a week or two longer, under wet antecedent conditions where the hydraulic response time governs. Under dry antecedent conditions at Alcove 1, the seepage duration is approximately 2 months shorter than the infiltration duration because of the delays arising from filling storage.

The Alcove 1 behavior implies that the end of each South Ramp seep corresponds to the end of the last precipitation event, and the longer lived seeps (more than 2 months in duration) also responded to the precipitation events occurring 2 months prior to the start of seepage. Tying the end of a seepage event in Figure 4-1 to the hydraulic response time, hydraulic response times for the seeps appear to range between 3 and 11 weeks. The onset of seepage appears to be linked to the precipitation events only 1 to 2 weeks earlier, but the longer lived seeps may have coincidentally just started responding to the earlier precipitation event as the later event occurred.

4.5 Local Distributed Infiltration Hypothesis

The local distributed infiltration hypothesis points to the mapped exposure of the nonlithophysal Tcpmn unit as the source of water, described in Figure 4-7 as the "local Distributed Source", with vertical flow in the inferred fault Day, et al. (1998) mapped providing the seep water at the high-volume seeps near station 75+95 and lateral flow in other faults moving some waters to the contiguous seep zone. As described in Section 4.3, the seep zone corresponds to the mapped exposure to within a few meters. This hypothesis implies that spatially distributed infiltration is focused into the faults to provide the seep waters.

The local distributed infiltration hypothesis implies that infiltration rates were sufficiently large in the nonlithophysal Tcpmn exposure to induce seepage, but not large enough to induce seepage in the lithophysal Tcpul exposure, consistent with a higher density of fractures in nonlithophysal units causing greater bulk bedrock permeability. The hypothesis implies that infiltration occurred on the top of the ridge and infiltrating waters are focused into discrete pathways with large seep rates. If appreciable net infiltration is limited to nonlithophysal units, waters forming the damp spot at station 76+32 must have moved laterally at least 25 m [80 ft].

The mechanism for increasing chloride concentrations by two to three orders of magnitude between the surface and the seep locations is not understood. Chloride may be stored in the soil profile or bedrock as previous wetting pulses dried out, or near the ESF as a result of ventilation, but the soil is so thin along the ridgetop that bedrock is exposed in locations (Stothoff, 2008b). Oliver and Whelan (2006) assert that the chemistry of the seep water is similar to unpublished measurements from the matrix near the seeps, implying that the seep waters may have passed through the matrix between the surface and the ESF or that the matrix water is the result of previous infiltration pulses with similar chemistry.

The local distributed infiltration hypothesis relies on the location of the nonlithophysal outcrop being close to the mapped location of the Tcpmn along the ridgetop. Subsequent field observations (Stothoff, 2008b) suggest that a lithophysal unit covers the ridgeline to a depth of 1 to 2 m [3.3 to 6.7 ft] at a U.S. Department of Energy-surveyed stake marking the primary seep location (i.e., station 75+95), with a nonlithophysal unit exposed down the ridgeline. Subsequent analysis of aerial photographs suggests that the contact between lithophysal and nonlithophysal units is approximately 5 m [16 ft] down the ridge from the primary seep location, implying that the actual exposure of the Tcpmn may be offset by approximately 30 m [100 ft] down the ridge from the mapped location.

Day, et al. (1998) asserts that the vertical accuracy of mapped unit contacts is within 1.5 m [5 ft]; this corresponds to a lateral extent of approximately 5 m [16 ft] at the slope of the ridgeline above the primary seepage zone. Day, et al. (1998) describe the field mapping process as

compiling field observations on mylar copies of base maps comprising topographic maps {10-ft [3.048-m] contour interval} overlain on a 1:6,000 orthophoto image; these observations were subsequently digitized. Black and white aerial photographs were used for the 1:6,000 scale orthophotos, according to planning documents (e.g., Blanchard, 1989), and the documents cite accuracy requirements such that 90 percent of the principal planimetric features are plotted to within 0.508 mm [0.02 in] of their true position, corresponding to 3 m [10 ft] at a 1:6,000 scale. Day, et al. (1998) does not provide the source of the topographic map; the documents planning the orthophoto missions (e.g., Blanchard, 1989) refer to a U.S. Geological Survey-digitized set of 10-ft [3.048-m] contours derived from U.S. Geological Survey 1:24,000 scale topographic quadrangles. Day, et al. (1998) do not discuss the accuracy of digitizing the drawn unit-contact lines, but it is likely within a millimeter, corresponding to approximately 6 m [20 ft].

The cumulative effect of inherent mapping and digitizing errors implies that contacts digitized from 1:6,000 scale maps may not be reliable at scales of less than approximately 9 m [30 ft], even if the contacts were drawn without error on the base map. In addition, the Tcpul and Tcpmn units are difficult to distinguish even on color photographs along this ridge, and the ridgeline at ESF station 75+95 is visually similar to the ridgeline at ESF station 76+25 in some photographs. In this area of this particular ridge, the unit contacts may have been identified correctly but shifted upslope by approximately 30 m [100 ft] on the black and white orthophoto.

In summary, the locally distributed infiltration hypothesis precisely matches seep locations to the contacts of the Tcpmn unit as mapped by Day, et al. (1998), but implies downdip subsurface lateral movement to account for the damp spot observed during construction at station 76+32. The hypothesis implies that (i) distributed infiltration is greater in nonlithophysal units than in lithophysal units, (ii) distributed infiltration occurs on ridgetops, (iii) distributed subsurface flow can focus into faults, and (iv) at least limited lateral downdip movement of water occurs. This explanation may be questionable for the deeper seep locations because the actual unit contacts appear to be displaced sufficiently far down the ridgeline from the mapped locations that the inferred flow pathways do not intersect the exposure of nonlithophysal tuff. However, the local distributed infiltration hypothesis offers an explanation for the damp spots observed during construction at stations 76+08 and 76+32 if the nonlithophysal unit is displaced down the ridgeline.

4.6 Channel Infiltration Hypothesis

The channel infiltration hypothesis recognizes that two intermittent channels exist in the area, both at a higher elevation than the seep locations. The nearer channel is offset horizontally by less than 30 m [100 ft] from the seep locations. Day, et al. (1998) map the Tcpmn unit as exposed in the channel close to the seep locations, and field observations (Stothoff, 2008b) found that the channel is incised into a densely fractured nonlithophysal reach with little or no soil near the seep locations. Farther upslope, the channel is incised into lithophysal rock. In the channel infiltration hypothesis, overland flow concentrates runoff from upslope exposures of the low-infiltration Tcpul unit, which then flows into a focused infiltration zone where faults intersect the channel bottom and the Tcpmn unit is exposed within the channel. Figure 4-7 uses “Channel Source” to illustrate this hypothesis. Channel flow durations are expected to be short because the catchments are small, on the order of 200 m [660 ft] upslope and 100 m [330 ft] across. To explain seepage at the ESF, the channel infiltration hypothesis does require that

waters spread laterally within fractures and faults from local infiltration sources at the channel bottom in order.

The channel infiltration hypothesis does not require a subsurface focusing mechanism to concentrate water into faults, unlike the distributed infiltration hypothesis. Projections of the seepage-related faults mapped in the ESF intersect the channel bottom in the reach where the channel is closest to the ESF.

The channel infiltration hypothesis explains high subsurface flows using mechanisms promoting near-surface lateral flow. As noted in Section 4.2, damp spots were observed below the PTn during ESF construction wherever mapped faults are exposed along the base of a hill slope above the ESF, implying that near-surface lateral redistribution provides sufficient additional water to these discrete features that relatively high fluxes could pass through the PTn within the fault zones. Although these locations may also feature redistribution in the soil column, upgradient reaches associated with the fault-related damp spots are comparable to the upgradient reach of the South Ramp channel.

The channel infiltration hypothesis implies that the standard chloride mass balance approach to estimating recharge fraction may not apply to interpreting seep waters. The standard chloride mass balance method assumes that all water and all chloride are limited to one flow pathway, which is not the case when near-surface lateral flow mixes many flow pathways. The chemistry of the waters entering the subsurface would reflect interactions with the soil during overland flow, and thus may not be directly comparable to the effective concentration (including wet and dry deposition) of precipitation. Samples of runoff elsewhere at Yucca Mountain (CRWMS M&O, 2003) typically have chloride concentrations approximately an order of magnitude larger than the effective concentration of precipitation. If runoff has similar chloride concentrations at this location, approximately an order of magnitude less evaporation would be required to explain the observed seepage concentrations than is necessary for the distributed infiltration hypothesis.

Under the channel infiltration hypothesis, the chemistry of the seep waters reflects near-surface interactions over the upslope watershed, and differences in chemistry at different seep locations are primarily due to evaporation and interactions with the rock mass after infiltration. The longer flow path contacting soils in the channel infiltration hypothesis implies that the water chemistries would be more affected by soil interactions relative to the distributed infiltration hypothesis. Although less altered by soil interactions, seep chemistry would generally be expected to be more heterogeneous under the distributed infiltration hypothesis, reflecting different soil and near-surface conditions. However, soil interactions on the ridgetop are likely to be spatially similar based on field observations (Stothoff, 2008b) that suggest that the soil is generally less than 10 cm [4 in] deep along the ridgetop and predominantly dominated by eolian deposition.

The channel infiltration hypothesis implies that some portion of the subsurface flows spreads laterally from the channel to contact the ESF, even though most flow may move in the steepest direction within the fault and fracture system. Spreading may be induced by capillary forces or irregularities and obstructions that cause resistance to flow. The maximum angle from vertical for the channel bottom to the crown of the ESF for observed seeps is approximately 27° at station 76+00, as described in Section 4.3. Seeps farther from the South Portal are deeper below the channel; thus the spreading angle is smaller. The damp spots closer to the South Portal have a larger spreading angle, so these are poorer candidates for the channel hypothesis. The southern channel is lower than the ESF crown at the secondary seep location,

although spreading may occur in a mapped fault lying within a small channel down the side of the ridge at the secondary seep location.

Several tests at Yucca Mountain provide comparative results related to lateral movement into fracture systems in densely welded tuffs. The Alcove 8/Niche 3 ponded infiltration test into fractures in the Ttpul and Ttpmn units exhibited wetness at the end of lateral borehole BH4, approximately 22.3 m [73.2 ft] below the infiltration gallery and 6.1 m [20 ft] laterally from the outside edge of the infiltration gallery (Salve, 2005). This configuration implies that lateral movement occurred with an unknown angle from the vertical of more than 15°, with an unknown extent of wetness beyond the end of the borehole. The Alcove8/Niche 3 observations imply that wet conditions were local features within the observation area, however, because Salve (2005) does not report wet conditions in other boreholes with similar configurations. In a ponded infiltration test at the site of the Large Block Test near Fran Ridge, Glass, et al. (2002) reported dye observations within the Tcpmn unit. This implies that dye traveled in the fracture system at least 3.5 m [11.5 ft] laterally from the edge of the pond to Level 8, approximately 3.5 m [11.5 ft] below the application horizon, yielding a maximum observed angle from the vertical of approximately 45° within the fracture system (although at most levels, maximum angles were approximately half of this maximum angle). Asymmetric spreading about the source was observed in both of these tests. Injection tests from a horizontal borehole into fractures in the Ttpmn unit at Alcove 6 (Salve, et al., 2002) consistently exhibited responses in two horizontal boreholes, 3 m [9.8 ft] lower, that imply responses at an angle greater than 45° from the nearest injection point.

In summary, the channel infiltration hypothesis explains the primary seepage locations (and perhaps the secondary seepage location) as a result of short-duration but large infiltration pulses from a reach of a small channel intersected by faults and exhibiting densely fractured exposed rock. The hypothesis does not fully account for the concentrated chemistry of the seepage water, although the infiltrating waters may be more similar to the seepage water chemistry than is the case for the local infiltration hypothesis. The hypothesis implies that lateral spreading occurs within the rock mass to explain seepage. Observations of analogous conditions provide limited corroboration that water can spread at the implied angle of spreading in a fractured tuff. The mechanism of flow focusing due to near-surface lateral flow into faults may also explain fault-associated damp spots found within the ESF below the PTn. The damp spots found at stations 76+08 and 76+32 may also be explained by channel infiltration, but would require shallower spreading angles that are not as well supported by corroborative observations. Although the short-duration seepage locations are consistent with a short-duration infiltration pulse, the Alcove 1 test suggests that long-duration seeps are not expected to result from short-duration channel infiltration in a fractured rock system with little storage.

4.7 Downdip Diversion Hypothesis

The downdip diversion pathway hypothesis links the source location to distributed infiltration upslope of the seep locations, with the infiltrating waters inferred to be diverted downdip within the Tcpmn unit or along the contact with the Tcpll (where present) and Tcpln units at the base of the Tcpmn unit. Figure 4-7 uses “Updrip Source” to illustrate this hypothesis. The Tcpmn crops out approximately 250 to 300 m [820 to 1000 ft] updip, marking the farthest geometrically possible downdip diversion distance, and the crest of the ridge is approximately 200 m [650 ft] updip. A long lateral travel path implies that the waters have more opportunity to interact with

the rock and pore waters than would be the case with a vertical travel path and would have the opportunity for mixing with high-chloride waters infiltrating in low-infiltration units along the pathway, consistent with observations that the seep water chemistry is similar to the pore-water chemistry. The downdip diversion hypothesis is consistent with the observation that the relatively high volume, long-lived seeps occurred where the Tcpmn/Tcpln contact intersects the crown of the ESF. Within the Tcpmn unit, a set of potential downdip pathways are provided by numerous laterally extensive vapor-phase partings, or cooling joints without macroscopic apertures lying approximately parallel to the base of the unit. This hypothesis implies that downward leakage across the base of the Tcpmn unit does not divert all water moving through the system from updip.

The as-built full periphery map of the South Ramp between stations 76+00 and 77+00 (Eatman, et al., 1997, Drawing OA–46–293), describing the lower half of the Tcpmn unit, identifies long subhorizontal features aligned with the base of the unit, indicated by roughly parabolic traces parallel to the Tcpmn/Tcpln contact. Figure 4-8 reproduces the section of the as-built map between stations 76+00 and 76+40; the Tcpmn and Tcpln units are labeled Tpcpmn and Tpcpln in the nomenclature used by Eatman, et al. (1997). These features with parabolic traces appear to correspond to features recorded as vapor-phase partings in the detailed line survey. The database capturing the detailed line survey, as Smart, et al. (2006) described, contains 88 features described as vapor-phase partings between stations 76+06 and 77+85. The same database records a total of 135 features described as vapor-phase partings in the remaining 7,634 m [25,045 ft] of the ESF.

Eatman, et al. (1997, Plate 1) suggests that this reach cuts through almost the entire thickness of the Tcpmn unit, which is approximately 60 m [200 ft] thick in this area. The detailed line survey recorded minimum and maximum apertures for each feature to the nearest millimeter. Five of the 88 partings (5.7 percent) had a nonzero recorded aperture, with a maximum of 11 mm [0.43 in]. Almost half of the features described as fractures, cooling joints, faults, and shears in this reach had a nonzero recorded aperture, with a maximum recorded aperture of 80 mm [3.1 in], implying that the vapor-phase partings tend to have relatively narrow apertures compared to other features. Similar vapor-phase partings are identified in the North Ramp exposure of the Tcpmn unit and in exposures of the analogous Ttpmn unit. Including the North Ramp exposures, 8.8 percent of all features identified as vapor-phase partings in the Tcpmn unit in the ESF have nonzero reported maximum apertures, and less than 3 percent have nonzero reported minimum apertures (all in the North Ramp, all with reported minimum apertures at the smallest nonzero increment). The detailed line survey more rarely identifies features as vapor-phase partings in other units.

The Alcove 1 water velocity is approximately 0.4 m/d [1.3 ft/d], assuming a travel time of 75 days and a travel distance of 30 m [100 ft], but the hydraulic response velocity is approximately 2 to 15 m/d [6.2 to 50 ft/d], assuming a hydraulic response time between 2 and 16 days. Assuming that the hydraulic response time is 75 days over the longest pathway for the long-lived South Ramp seeps, 300 m [100 ft], the hydraulic response time would be 4 m/d [13 ft/d], corresponding to an intermediate hydraulic response time of 8 days in the Alcove 1 experiment. Seeps ending 21 days after the last precipitation event would have hydraulic response times of 14 m/d [46 ft/d] at the extreme upper end of the Alcove 1 range, representing the initial response to a large infiltration pulse.

Interpreting the seepage response times as a hydraulic response over 300 m [1,000 ft] appears to be consistent with the Alcove 1 observations for the long-duration seeps and is at the edge of

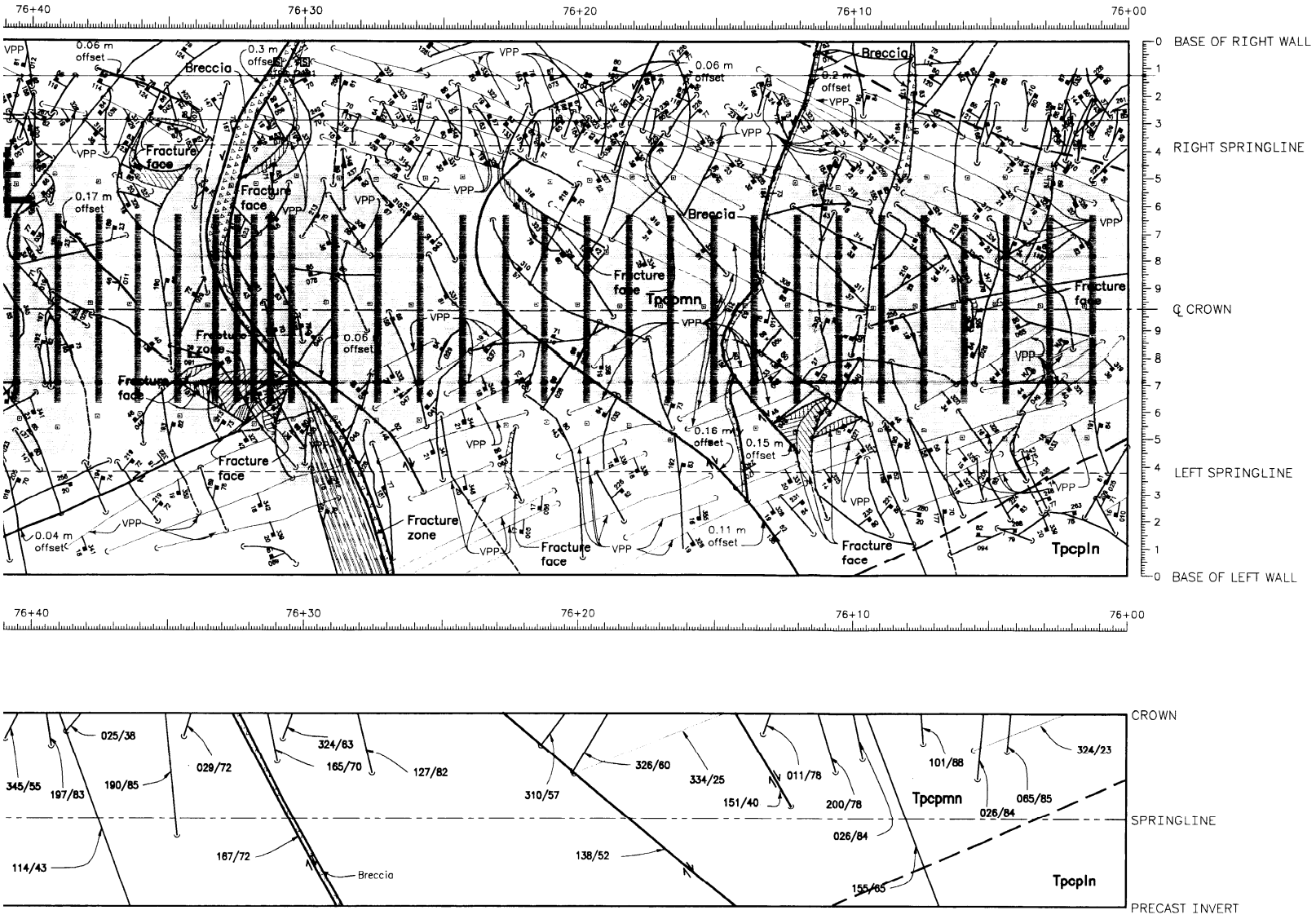

Figure 4-8. Section of As-Built Full-Periphery Map Between Exploratory Studies Facility Stations 76+00 and 76+40 (Reproduced from Eatman, et al., 1997, Drawing OA 46 293)

consistency for the short-duration seeps. However, interpreting the seepage response times as a travel time over this distance implies that the water moved 10 times faster than for the Alcove 1 experiment with a gravity driving force approximately one-third as large (assuming a dip angle of 20°). which appears to be inconsistent with the Alcove 1 observations. Accordingly, the downdip diversion hypothesis implies that the infiltrating waters only traveled a fraction of the distance to the seepage location, displacing waters already in place. If so, travel times are longer than the duration of the seepage event, numerous events would be necessary to move infiltrating waters to the seepage location, and the waters would have greatly increased opportunity to interact with the rock and pore waters.

The downdip diversion hypothesis also implies that there is little delay to fill storage in order to achieve the relatively rapid hydraulic response times; thus the hydraulic pathway must be largely preserved between flux events. This in turn implies that the predominant pathways for response must remain almost saturated, which requires that the pathways have relatively narrow apertures so that capillary forces retain water in the pathway. As described previously, vapor-phase partings appear to have relatively narrow apertures, consistent with hypothesis requirements.

Subvertical fractures tend to have larger apertures than the vapor-phase partings, which makes subvertical fractures act as capillary barriers to lateral flow and conduits for gas movement. However, if the vapor-phase partings are more laterally extensive than the subvertical fractures, water in the vapor-phase partings will tend to flow around the subvertical fractures. Even so, some percentage of the flow in the vapor-phase partings would divert into subvertical fractures; thus water would tend to move downward, implying that extensive lateral diversion would predominantly occur just above a barrier blocking hydraulic transfer through the subvertical fracture network. If the fracture system is largely stratabound at the Tcpmn/Tcpll or Tcpmn/Tcpln contacts, the contact zone may have bulk permeability orders of magnitude smaller than the unit as a whole and thereby restrain downward liquid flow in the fracture system. Because the gas phase moves much more readily than the liquid phase through the fracture system, a sparse set of discontinuities in a thin barrier may propagate barometric pulses through the barrier but only slowly allow a liquid pulse to pass through. The full periphery map of the South Ramp (Eatman, et al., 1997, Drawings OA –46–282 and OA–46–293) indicates that the fracture patterns are distinctly different in the Tcpln and Tcpmn, but it is not clear that the fracture systems are stratabound, and the Tcpmn/Tcpll contact is not observed in the South Ramp.

All of the seeps underlie the lowest mapped vapor-phase parting in the Tcpmn. The seep locations within the Tcpln unit are associated with faults that are aligned to intercept the Tcpmn subhorizontal discontinuities. Under the downdip diversion hypothesis, these faults would be examples of breaks in the barrier where water is leaking through. The damp spots at the contact between the Tcpln and PTn at stations 74+95 and 75+00 may represent the remnants of waters leaking through the Tcpmn/Tcpln barrier during previous events, and the damp spots at stations 76+08 and 76+32 may also be explained by prior downdip water movement.

In summary, the downdip diversion hypothesis is consistent with laterally extensive narrow-aperture subhorizontal discontinuities immediately above a contact with largely stratabound fracture sets. In this situation, the lowest subhorizontal discontinuities remain largely saturated, allowing hydraulic responses to quickly propagate through the system, but the actual water may travel a much shorter distance during a seepage event. In this situation, the waters have long residence times within the unsaturated zone, allowing extended interaction

between the rock and pore waters. The downdip hypothesis appears to better describe long-duration seeps than short-duration seeps.

4.8 Summary

The seepage event in the South Ramp starting in the winter of 2005 provides information related to the infiltration pathways that may operate at other locations. The observations described in Section 4 suggest three hypothetical sources and pathways for the seep water in the primary seepage zone (i.e., between stations 75+60 and 76+04) as illustrated in Figure 4-7. The predominantly vertical local distributed infiltration pathway recognizes that the seeps are essentially coincident with the extent of overlying mapped Tcpmn unit exposures. The channel infiltration pathway recognizes that two intermittent channels exist in the area, with both at a higher elevation than the seep locations and with the nearer channel offset horizontally by approximately 30 m [100 ft] from the seep locations. The downdip diversion pathway recognizes that the seeps occur near a contact between the overlying Tcpmn and underlying Tcpln unit, with the Tcpll unit pinching out some unknown distance updip. None of these lithologic configurations occurs in any other stretch of the ESF.

The local distributed infiltration pathway hypothesis links the source location for the seep waters to a gap in the Tcpul exposure along the ridgetop above the South Ramp indicated on the Day, et al. (1998) 1:6,000 scale central block bedrock map. This gap exposes the underlying Tcpmn unit, which Stothoff (2008a) links to relatively larger infiltration than the Tcpul unit because of greater fracture density. The mapped Tcpul/Tcpmn contacts tightly bound the inferred source area for the seeps under predominantly vertical flow. However, field observations using a U.S. Department of Energy-surveyed location (Stothoff, 2008b) and subsequent analysis suggest that the mapped gap may be displaced upslope by approximately 30 m [100 ft] relative to the seep location. If the gap were located 30 m [100 ft] downslope, neither vertical flow nor flow along inclined faults would explain the full extent of the seepage zone, but damp spots nearer the South Portal that were found during ESF emplacement and are otherwise unexplained would lie under the gap. The chemistry of the seep water is two to three orders of magnitude more concentrated than inferred effective concentrations for precipitation, implying that the waters experienced rapid and substantial increase in dissolved-species concentration under the locally distributed pathway.

The channel infiltration pathway hypothesis links the source location for the seep waters to a channel incised into the Tcpmn unit approximately 30 m [100 ft] to the south of the ESF. The channel has extensive exposure of densely fractured bedrock at the channel; faults mapped in the ESF project into the channel; and relatively impermeable Tcpul exposed over most of the contributing catchment. This hypothesis is consistent with the observation that damp spots in the ESF below the PTn are consistently found where mapped faults are oriented along the base of hillslopes. The hypothesis may not explain the damp spots nearer the South Portal, because the angle between the channel bottom and the crown of the ESF becomes less vertical nearer the South Portal. Major ion concentrations in runoff are elevated relative to precipitation, because overland flow brings the waters into contact with the soil; therefore the waters entering the ground in the channel infiltration hypothesis may be closer to the observed seep water concentrations than would be the case in the distributed infiltration hypothesis. However, waters would need to move laterally with an angle from the vertical approaching 30°, and it is not clear that spreading would occur perpendicular to the dip direction at such an angle within faults. The channel infiltration pathway hypothesis explains short-duration seeps better

than long-duration pulses because there is relatively little storage in the fracture system to prolong percolation pulses.

The downdip diversion pathway hypothesis links the source location to relatively widespread distributed infiltration upslope of the seep locations, with the infiltrating waters inferred to be diverted downdip within narrow-aperture subhorizontal discontinuities in the Tcpmn along the contact at the base of the Tcpmn unit. This hypothesis is consistent with the observation that the relatively high volume, long-lived seeps occurred where the Tcpmn/Tcpln contact intersects the crown of the ESF and the observation that the Tcpmn unit features numerous, long, subhorizontal vapor-phase partings aligned with the bedding plane. The hypothesis is consistent with solute compositions that are similar to the pore waters, because the waters may have long residence times within the unsaturated zone. Pneumatic observations suggesting that barometric pressure changes are rapidly propagated through the entire TCw unit are consistent with a generally stratabound fracture system restricting vertical liquid flow at the contact if pneumatic pulses are propagated through relatively few scattered high-capacity pathways. The downdip diversion pathway hypothesis explains long-duration seeps better than short-duration pulses because short-duration pulses respond more quickly than is consistent with the Alcove 1 experiment.

The set of seeps and damp spots may result from a combination of the three hypothesized pathways. In particular, a mix of short- and long-duration seeps would result from a combination of the channel and downdip diversion pathways. Further, changes in chemistry over relatively short distances would be explained by mixing between two different sources of infiltrating waters with much different residence times in the subsurface. On the other hand, local infiltration may be a more readily explainable pathway for certain damp spots than either the channel or downdip diversion pathways.

In summary, the primary seep locations may be a result of combined factors not found above the ESF and ECRB at any other location. The seeps occurred above the PTn, which is thought to reduce fracture flows by drawing water from the fracture system into the matrix as a result of capillary forces; only a relatively short stretch of the ESF lies above the PTn, in the North and South Ramps, and in the North Ramp approximately half of this length is overlain by alluvium. Further, the seeps are located at and near a fault that intersects a nearby channel (to the south) in the Tcpmn zone where the channel is closest to the ESF. The channel and hillslope near the channel are densely fractured, the channel has exposed bedrock, and most of the upslope catchment has shallow soil overlying the relatively less fractured and low permeability Tcpul. These factors are relatively conducive to both direct infiltration and lateral flow from channel infiltration. The seeps are also associated with a contact between welded units, and the overlying unit has properties that may favor lateral diversion above a contact with stratabound fractures. This may be the only unit contact between welded units above the PTn that has the same properties, although an analogous situation of lateral flow in a stratabound fracture system may occur at the moderately welded transition between the TCw and PTn and analogous unit contacts may occur in the TSw.

.